Lai, Yong; Wu, Kuowei

A New 3D Hydrostatic-assumption Model for Turbidity Current Simulation

12th International Conference on Hydroscience & Engineering
Hydro-Science & Engineering for Environmental Resilience
November 6-10, 2016, Tainan, Taiwan.

A New 3D Hydrostatic-Assumption Model for Turbidity Current Simulation

Yong Lai[1], *Kuowei Wu*[2]
1. Technical Service Center, U.S. Bureau of Reclamation
Denver, Colorado, USA
2. Water Resources Planning Institute, Water Resources Agency
Wu-Fong, Taichung, Taiwan

ABSTRACT

3D hydrostatic-assumption (HA) models have been widely used in environmental flows where 3D effect is important but hydrostatic assumption is sufficiently valid. This is the case for most eco-hydraulic issues in reservoirs. This study reports the research and development of a new 3D HA model named SRH-3D suitable for turbidity current simulation in reservoirs. SRH-3D adopts a new mesh type and new numerical algorithms. In the paper, a brief review is provided with regard to the existing 3D HA models along with shortcomings. The governing equations and the new numerical methods are then presented for turbidity current simulation. Selected test cases are reported to show the capability of the new model.

KEY WORDS: Turbidity Current; 3D Model; Hydrostatic Assumption; Reservoir Sedimentation

INTRODUCTION

There are many instances where one-dimensional (1D) and two-dimensional (2D) depth-averaged models are insufficient for environmental modeling. One such example is turbidity currents in reservoirs. A 2D layer-averaged model has been developed by Lai et al. (2015) for reservoir turbidity current modeling; but limitations have been found when sediment sluicing needs to be modelled. The need for three-dimensionality led to the development of three-dimensional (3D) environmental fluid dynamic (EFD) models. In theory, non-hydrostatic 3D EFD models are the most general and accurate, subject mainly to the accuracy of turbulence and relevant physical models. However, these EFD models are yet to be practical for large scale environmental flows due to prohibitive requirements of computing power or difficulties in using the models. A good alternative is to evoke the hydrostatic assumption, leading to the development of 3D hydrostatic-assumption (HA) models. These models are much easier to use, fast in simulation turn around, and have the potential for most practical applications.

This study reports the research and development of a new 3D HA model, named SRH-3D. The new model aims to achieve the following objectives: (a) to develop a 3D HA model suitable for field simulation of turbidity currents in reservoirs on a desktop PC; and (b) to design numerical methods that may overcome some shortcomings of the existing 3D HA models.

A BRIEF REVIEW

Many 3D HA models have been developed for lake, reservoir and oceanic and costal simulation. Examples include ECOMSED, RMA10, GBTOXe, EFDC3D, ROMS, CH3D-SED, and Delft3D, among others. Readers may refer to the review by Papanicolaou et al. (2008). Following models have been reviewed with more details in the present study: POM and ECOMSED (Blumberg and Mellor 1983; 1987); Delft3D-Flow (Roelvink and van Banning 1994; Lesser 2000); EFDC3D (Hamrick, 1992); and CH3D-WES (Johnson et al., 1993; Spasojevic and Holly, 1994; Gessler et al., 1999). It is found that most 3D HA models adopt curvilinear structured mesh horizontally and either sigma-grid or Z-grid vertically. For example, Delft3D-Flow uses an orthogonal quadrilateral mesh horizontally and sigma-grid or Z-grid vertically.

The mesh system used by existing models is one of the weaknesses. Structured horizontal mesh is not easy to generate and often inefficient for representing complex terrains and bathymetry. Vertical mesh method has its own pitfalls. The sigma-grid transforms the governing equations from physical space to computational space. It has the benefit of fixed free surface and bed elevation representation; however, it encountered many problems. For example, it might not have the adequate resolution around a density interface causing significant errors in the modeling of horizontal density gradients in areas with steep bottom topography (Leendertse, 1990; Stelling and van Kester, 1994). The Z-grid was developed to overcome the problems of the sigma-grid and to simulate the weakly forced stratified water systems. The Z-grid uses the physical-coordinates that avoided equation transformation. The vertical point distribution, however, is not arbitrary and its co-ordinate lines are horizontal. Different number of vertical points is used in different areas and grid lines are nearly parallel with density interfaces. However, the Z-grid is not boundary-fitted in the vertical direction so bed is represented using staircase approximation. The zig-zag representation was found to lead to high inaccuracies in computing bed shear stress and horizontal advection near beds (Bijvelds 2001; Cornelissen 2004).

In this study, a new mesh system is proposed: an unstructured and physical-coordinate (UPC) mesh. A UPC mesh adopts unstructured arbitrarily shaped cells in the horizontal plane and an equal number of physical-coordinate mesh points in the vertical direction. Key differences of the UPC mesh from the traditional sigma-mesh include:

(a) Horizontal mesh may assume any cell shapes such as mixed quadrilaterals and triangles; (b) the physical, Cartesian based governing equations are solved directly without coordinate transformation; and (c) vertical mesh points are allowed to conform to free surface and bed without staircase. With the proposed UPC mesh, a flexible 2D mesh is generated first using a 2D mesh generator; the 3D mesh is then generated automatically based on model predicted bed and free surface. Use of a 2D mesh eliminates the need for a 3D mesh generation that is both complex to apply and time consuming in applications.

GOVERNING EQUATIONS

SRH-3D makes the following assumptions: (a) vertical pressure distribution is hydrostatic; (b) the Boussinesque assumption is appropriate in which density variation impacts only the buoyancy force; and (c) the flow-sediment mixture is incompressible. We are concerned primarily with reservoirs so that coastal issues such as ocean wave generated processes and Coriolis force are not considered. The above assumptions lead to the following 3D HA flow equations:

$$\frac{\partial U}{\partial x}+\frac{\partial V}{\partial y}+\frac{\partial W}{\partial z}=0 \tag{1}$$

$$\frac{\partial U}{\partial t}+\frac{\partial UU}{\partial x}+\frac{\partial VU}{\partial y}+\frac{\partial WU}{\partial z}=-g\frac{\partial \zeta}{\partial x}-\frac{g}{\rho}\int_z^{\zeta}\frac{\partial \rho}{\partial x}dz' +\frac{\partial T_{xx}}{\partial x}+\frac{\partial T_{xy}}{\partial y}+\frac{\partial}{\partial z}\left((\upsilon+\upsilon_V)\frac{\partial U}{\partial z}\right) \tag{2}$$

$$\frac{\partial V}{\partial t}+\frac{\partial UV}{\partial x}+\frac{\partial VV}{\partial y}+\frac{\partial WV}{\partial z}=-g\frac{\partial \zeta}{\partial y}-\frac{g}{\rho}\int_z^{\zeta}\frac{\partial \rho}{\partial y}dz' +\frac{\partial T_{yx}}{\partial x}+\frac{\partial T_{yy}}{\partial y}+\frac{\partial}{\partial z}\left((\upsilon+\upsilon_V)\frac{\partial V}{\partial z}\right) \tag{3}$$

$$\frac{\partial \zeta}{\partial t}+\frac{\partial}{\partial x}\int_{Z_B}^{\zeta}Udz'+\frac{\partial}{\partial y}\int_{Z_B}^{\zeta}Vdz'=0 \tag{4}$$

In the above, t is time; (x, y, z) are the Cartesian coordinates with z the vertical direction; ρ is the water-sediment mixture density and can be a function of sediment concentration; U, V, W are the mean velocity components along the Cartesian coordinates x, y, z, respectively; g is the acceleration due to gravity; ζ is the free surface elevation; T_{xx}, T_{xy}, T_{yx} and T_{yy} are turbulence stresses in the horizontal direction; υ_V is the turbulent eddy viscosity in the vertical direction. Various turbulence models may be used to compute the turbulence stresses as well as the horizontal and vertical viscosities. They are presented by Lai and Wu (2016) and not repeated herein. In this study, the large eddy simulation (LES) model is used for horizontal turbulence and k-ε model is used for vertical turbulence.

SRH-3D turbidity current module solves the suspended load transport. The suspended sediment concentration is tightly coupled to the flow in that flow dictates sediment concentration distribution while suspended sediments alters the flow through the baroclinic term in the momentum equations. The coupling is the result of altered water mixture density due to the presence of sediment concentration.

All suspended sediments are divided into a number of size classes. Each size class is then transported according to the following advection-diffusion mass-balance equation:

$$\frac{\partial C_k}{\partial t}+\frac{\partial UC_k}{\partial x}+\frac{\partial VC_k}{\partial y}+\frac{\partial (W-\omega_k)C_k}{\partial z}= =\frac{\partial}{\partial x}\left(D_{Hk}\frac{\partial C_k}{\partial x}\right)+\frac{\partial}{\partial y}\left(D_{Hk}\frac{\partial C_k}{\partial y}\right)+\frac{\partial}{\partial z}\left(D_{Vk}\frac{\partial C_k}{\partial z}\right) \tag{5}$$

In the above, C_k is the volume concentration of sediment size class k; ω_k is the hindered fall velocity for size k; D_{Hk} and D_{Vk} are the horizontal and vertical diffusivities computed by:

$$D_{Vk}=\frac{\upsilon_V}{\sigma_{Ck}}; \qquad D_{Hk}=\frac{\upsilon_H}{\sigma_{Ck}} \tag{6}$$

In the above σ_{Ck} is the Schmidt parameter assumed to be a constant (0.5 to 1.0 based on Celik and Rodi 1988).

The suspended load equation (5) is solved with boundary conditions specified at free surface and near bottom walls. At free surface, the net sediment concentration flux is set to zero; i.e.,

$$\omega_k C_k + D_{Vk}\frac{\partial C_k}{\partial z}=0 \tag{7}$$

At stream bed, the net sediment flux reflects the sediment exchange between those in water and those on the bed; it is not zero unless the flow has reached equilibrium. The net flux out of water column is computed by:

$$\omega_k C_k + D_{Vk}\frac{\partial C_k}{\partial z}=D_k - E_k \tag{8}$$

where $D_k=\omega_k C_k$ and E_k are the sediment deposition and entrainment rates, respectively. The entrainment rate may be computed by

$$E_k=\begin{cases}\omega_k C_k^* & \text{loose bed with unlimted supply}\\ \min\left(\omega_k C_k^*, \omega_k C_k\right) & \text{fixed bed without supply}\end{cases} \tag{9}$$

In the above, entrainment is proportional to the local equilibrium concentration (C_k^*) near the bed. The equilibrium concentration is determined by the formula of Zyserman and Fredsøe (1994) as follows:

$$C^* = \frac{0.331(\theta - 0.045)^{1.75}}{1 + \frac{0.331}{0.46}(\theta - 0.045)^{1.75}} \quad (10a)$$

$$\delta = 2d \quad (10b)$$

$$\theta = \frac{u_\tau^2}{(\gamma - 1)gd} \quad (10c)$$

Numerical solution of the flow governing equations has been discussed in details by Lai and Wu (2016). The solution of the suspended equation, along with the boundary conditions, can be similarly done. They are not presented due to page limit.

MODEL TEST AND RESULTS

A number of cases have been selected to test and validate the new model and they are presented below

Channel Flow with Suspended Sediment

3D modeling of suspended sediment is not trivial; correct implementation of even the boundary condition near bed is not well understood as shown by Liu (2014). The channel flume results of Fuhrman et al. (2010) are used to test the near-wall flow and correct implementation of suspended sediment equation.

The experiment was carried out in a flume with rough bottom created by placing a single layer of pebble-sized stones (median diameter of 7 mm). The bed slope is 0.07252%. The water elevation from the roughened bottom was reported to be 62 mm after the flow is fully developed. A log-fit of the measured velocity profile led to the shear velocity $u_\tau = 0.021$ m. The mean velocity was 0.22 m/s. The numerical model used a horizontal mesh of 62-by-1 cells covering 12.4 m in length and 1 m in width. A total of 31 vertical cells are used and distributed non-uniformly. Finer points are near the free surface in order to make the first point near bed located within the log-law region. The cell center of the first cell near bed is $\delta_1 = 2.4415$ mm so that the point is within the log-law ($y^+ = \delta_1 u_\tau / \nu = 53.4$). Upstream discharge is 0.01364 m^3/s; downstream depth is 62 mm; bed roughness height is $k_s = 13$ mm.

The computed velocity and vertical eddy viscosity distribution are compared with experimental data in Figure 1. Good results are obtained. Vertical eddy viscosity is important in predicting the suspended sediment transport. For the present case, only two mechanisms are important for sediment motion: settling velocity and turbulent resuspension. The well-cited experimental data sets from Ueda et al. (1977) and Nezu and Rodi (1986) are used for comparison of turbulent viscosity.

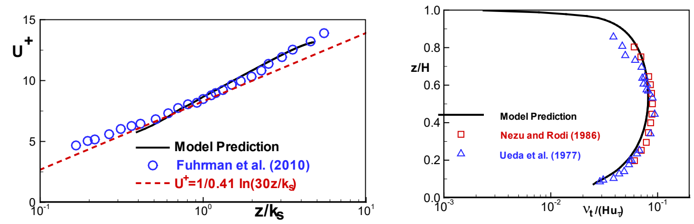

(a) Velocity (b) Turbulent Viscosity

Fig. 1 Comparison of predicted results with the measured data

Two runs are made for suspended sediment prediction with two sediment sizes; the same runs were reported by Liu (2014). The parameters of the two runs are in Table 1. The sediment sizes were chosen such that the Rouse parameters $\beta = \omega_s / (0.41 u_\tau)$ are significantly different. The simulation starts from clear water and stops once the equilibrium sediment concentration profiles are obtained. Predicted concentration is compared with the theoretical Rouse profile in Figure 2. The agreement is good considering that the Rouse profile is only approximate and was derived by assuming the vertical turbulence viscosity is parabolic.

Table 1 Parameters of two suspended sediment runs

Run	d(mm)	ω_s (m/s)	C_{b^*}	Rouse β
1	.0236	5.16e-5	0.210	0.06
2	.0790	5.79e-3	0.036	0.672

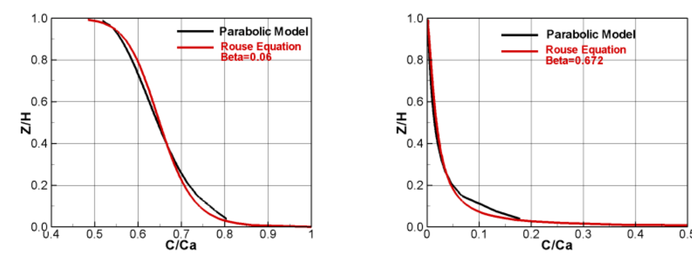

(a) Run 1 (b) Run 2

Fig. 2 Comparison of suspended sediment concentration

Lock Exchange: Intrusive Turbidity Current into a Two-layer Fluid

Intrusion of a gravity current into a two-layer fluid is simulated, corresponding to the experimental setup of Sutherland et al. (2004). The case is illustrated in Figure 3. The flume has a glass tank measuring 197.1 cm long by 19.9 cm wide by 48.5 cm tall. The lock-length (*l*) behind gate is 18.6 cm and the total water depth (H) is 20 cm.

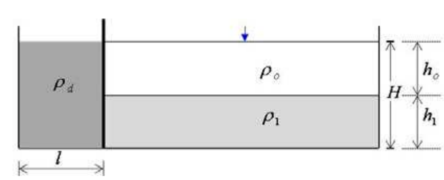

Fig. 3 Parameters for the intrusive gravity current (An 2011)

Two cases are simulated and compared with the available data. The first is a symmetric flow turbidity current in which the depth of the two layers in the ambient fluids is equal ($h_0 = h_1 = 10$ cm). The densities are: $\rho_0 = 1000$ kg/m^3, $\rho_1 = 1020$ kg/m^3, and $\rho_d = 1010$ kg/m^3. The case has the symmetrical flow type according to Sutherland et al. (2004) as the density of the lock fluid is equal to the depth-weighted average of the upper and lower layers. The second case is an asymmetric flow turbidity current in which the depth of the two layers in the ambient fluids is $h_0 = 17.5$ cm and $h_1 = 2.5$ cm. The densities are: $\rho_0 = 1000$ kg/m^3, $\rho_1 = 1020$ kg/m^3, and $\rho_d = 1015$ kg/m^3.

In modeling, symmetry is assumed in the lateral (y) direction while the two side boundaries are set up as the symmetry boundary condition. The mesh has 533 cells longitudinally (x) and 50 cells vertically (z). Initially, fluid is stationary. For the symmetric case, the initial concentration is $C = 0.006061$ in the lock, C = 0.0 and 0.012122, respectively, in the top and bottom of the ambient. For the asymmetric case, C = 0.009091 in the lock and C = 0.0 and 0.012122 in the top and bottom of the ambient

Simulation results of the symmetric case are shown in Figure 4 to visualize the temporal evolution of the intrusive gravity current. They are compared with images taken from laboratory experiments of Sutherland et al. (2004) and figures from a non-hydrostatic model reported by An (2011). After the lock gate is removed, the fluid contained behind the lock gate collapsed symmetrically and propagated along the interface. The head already started to form and is visible at 2 s. The initial collapse began with rapid acceleration. As it propagated to the right end of the wall, the gravity current brought strong mixing, resulting in mass entrainment and dilution. The results confirm the finding of Fringer et al. (2006) that hydrostatic model such as SRH-3D cannot predict the formation of the Kelvin-Helmholtz billows. However, the model is capable of predicting the overall features such as the propagation speed.

Simulated results of the asymmetric case are shown in Figure 5 with the temporal evolution of the intrusive gravity current displayed. Model results are compared with experiments of Sutherland et al. (2004) and 3D non-hydrostatic model results of An (2011). It is seen that the HA model is incapable of predicting the Kelvin-Helmholtz waves as well as the wave reflection phenomenon after the front reaches the end wall. However, the HA model predicts the current movement speed reasonably.

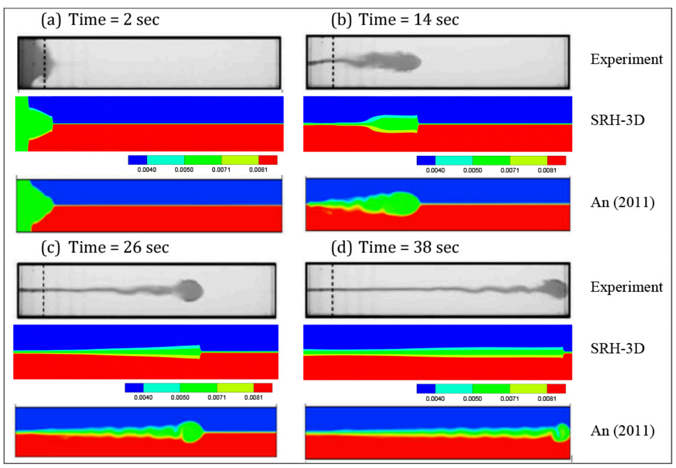

Fig. 4 Temporal evolution of the symmetric intrusive gravity current. Experiment is from Sutherland et al. (2004)

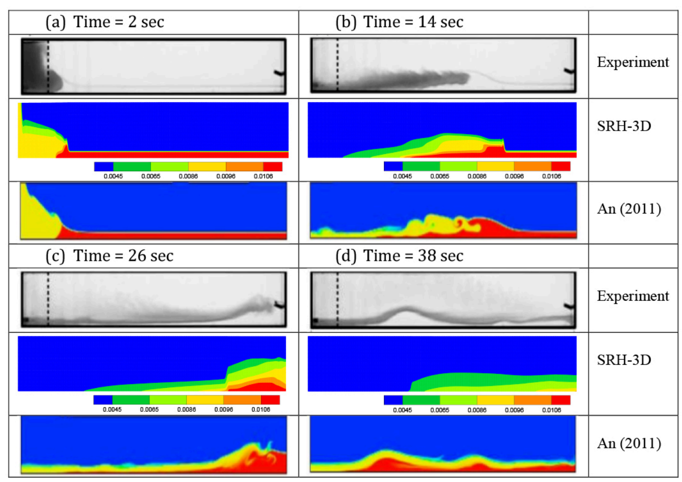

Fig. 5 Temporal evolution of the asymmetric intrusive gravity current. Experiment is from Sutherland et al. (2004).

CONCLUSIONS

A new 3D HA model, SRH-3D, has been developed to predict reservoir turbidity current. The model is tested and verified with selected cases. Despite the inability of predicting waves associated with the Kelvin-Helmholtz instability, 3D HA models are adequate to predict the overall features of turbidity current propagation.

REFERENCES

An, S.D. (2011). Interflow Dynamics and Three-Dimensional Modeling of Turbid Density Currents in Imha Reservoir, South Korea. Ph.D. Thesis, Department of Civil and Environmental Engineering, Colorado State University, Fort Collins, Colorado.

Bijvelds, M.D.J.P. (2001). Numerical modelling of estuarine flow over steep topography. Delft, Delft University of Technology.136 pp.

Blumberg, A.F. and Mellor, G.L. (1983). Diagnostic and prognostic numerical circulation studies of the south Atlantic bight. J. Geophys. Res., 88(C8): 4579-4592.

Blumberg, A. F. and Mellor, G.L. (1987). A description of a three-dimensional coastal ocean circulation model. In: N.S. Heaps (eds), Three-Dimensional Coastal Ocean Models, Coastal and Estuarine Science, Vol. 4. American Geophysical Union, pp. 1-19.

Celik, I. and Rodi, W. (1988) "Modeling suspended sediment transport in nonequilibrium situations." J. Hydraul. Eng., 114(10): 1157-1191.

Cornelissen, S.C. (2004). Numerical Modelling of Stratified Flows Comparison of the sigma and z coordinate systems. M.Sc. Thesis, Delft University of Technology. 94 pp.

Fringer, O. B, Gerritsen, M. G, Street, R. L (2006) "An Unstructured-grid, Finite-Volume, Nonhydrostatic, Parallel Coastal Ocean

Simulator." Ocean Modelling 14, 139-173.

Fuhrman, D. R., Dixen, M., and Jacobsen, N. G. (2010). "Physically-consistent wall boundary conditions for the k-omega turbulence model." Journal of Hydraulic Research, 48(6), 793-800.

Gessler, D., Hall, B., Spasojevic, M., Holly, F. M., Pourtaheri, H., and Raphelt, N. X. (1999). Application of 3D mobile bed, hydrodynamicsmodel. J. Hydraul. Eng., 125(7): 737-749.

Hamrick, J. M., (1992). A Three-Dimensional Environmental Fluid Dynamics Computer Code: Theoretical and Computational Aspects. The College of William and Mary, Virginia Institute of Marine Science. Special Report 317, 63 pp.

Johnson, B.H., K.W. Kim, R.E. Heath, B.B. Hsieh, and H.L. Butler, (1993). Validation of three dimensional hydrodynamic model of Chesapeake Bay. J. Hydraul. Eng. 119: 2-20.

Lai, Y.G., Huang, J. and Wu, K. (2015). "Reservoir Turbidity Current Modeling with a Two-Dimensional Layer-Averaged Model." J. Hydraulic Engineering. Vol.141(12). 04015029 1-15.

Lai, Y.G. and Wu, K. (2016). "A new 3D hydrostatic-assumption model for river and reservoir modelling." River Flow 2016, 8th International Conference on Fluvial Hydraulics, St. Louis, Mo. July 12-15, 2016.

Leendertse, J.J., (1990). Turbulence modelling of surface water flow and transport: part IVa. J. Hydraul. Eng. 114(4): 603-606.

Lesser, G. R. (2000). Computation of three-dimensional suspended sediment transport within the DELFT3D-FLOW module. WLjDelft Hydraulics report Z2396, Delft, 123 pp.

Liu, X. (2014). "New Near-Wall Treatment for Suspended Sediment Transport Simulations with High Reynolds Number Turbulence Models." J. Hydraul. Eng., 140(3), 333-339.

Nezu, I., and Rodi, W. (1986). "Open-channel flow measurements with a laser doppler anemometer." J. Hydraul. Eng., 10.1061/(ASCE)0733-9429(1986)112:5(335), 335-355.

Papanicolaou, A.N.T., Elhakeem, M., Krallis, G., Prakash, S., Edinger, J. (2008). Sediment Transport Modeling Review - Current and Future Developments. J. Hydraul. Eng. 134(1): 1-14.

Roelvink, J.A., and van Banning, G.K.F.M. (1994). "Design and development of DELFT3D and application to coastal morphodynamics." In Hydroinformatics, ed. A Verwey, AWMinns, V Babovic, C Maksimovic, pp. 451-56. Rotterdam: Balkema.

Spasojevic, M., and Holly, F. M. (1994). Three-dimensional numerical simulation of mobile-bed hydrodynamics. Contract Rep. HL-94-2, U.S. Army Engineer Waterways Experiment Station, Vicksburg, Miss.

Stelling, G.S. and J.A.Th.M. van Kester, (1994). On the approximation of horizontal gradients in sigma co-ordinates for bathymetry with steep bottom slopes. Int. J. Num. Meth. Fluids 18: 915-955.

Sutherland, B. R., Kyba, P. J., and Flynn, M. R. (2004). "Intrusive Gravity Currents in Two-layer Fluids." Journal of Fluid Mechanics, 514, 327-353.

Ueda, H., Moller, R., Komori, S., and Mizushina, T. (1977). "Eddy diffusivity near the free surface of open channel flow." Int. J. Heat Mass Transfer, 20(11), 1127-1136.